RSC Advances

PAPER

View Article Online
View Journal | View Issue

Cite this: *RSC Adv.*, 2015, **5**, 12261

A special Ag/AgCl network-nanostructure for selective catalytic degradation of refractory chlorophenol contaminants†

Zaidi Huang,[a] Ming Wen,*[ab] Dandan Wu[a] and Qingsheng Wu*[a]

Received 13th November 2014
Accepted 23rd December 2014

DOI: 10.1039/c4ra14459g

www.rsc.org/advances

A special Ag/AgCl network-nanostructure was synthesized based on a Ag nanowire (NW) or nanosphere template through the element lithographic network construction process. The structure of obtained Ag/AgCl is a 3D nanoscale network-structure that consists of the network NWs with the average diameter of ~20 nm and porous channels with narrow macropore distribution from 50 to 100 nm. As-designed network-nanostructures not only provide firm frame support for the active sites, but also offer large surface areas and numerous reaction performance chambers, and consequently greatly facilitate reactant diffusion and transport. Employed as UV-driven plasmonic photocatalysts, the formulated Ag/AgCl nano-networks exhibit excellent performance and stability for the selective degradation of chlorophenol contaminants. Compared with the commercial P25-TiO_2, the prepared Ag/AgCl network-nanostructures show considerably higher photocatalytic activity, in which the network-structured nanospheres are better than network-structured NWs toward the selective degradation of 4-chlorophenol with the reaction rate constant of 0.28 min^{-1}, suggesting good potential application for organic pollutant elimination.

Introduction

In environmental management, it is difficult to degrade the toxic organic contaminants because a lot of them are resistant to conventional chemical and biological treatments. Chlorophenol aromatic compounds are one of the most refractory pollutants existing in industrial effluents, especially 4-chlorophenol (4-CP), which is carcinogenic, mutagenic, teratogenic, nonbiodegradable and highly toxic. Thus, catalytic degradation as a sustainability approach can reduce the negative impacts on water bodies and benefit the reuse and regeneration.[1–3] To date, some TiO_2-based catalysts have been developed for the photodegradation of the organic pollutants.[4–14] However, it is still difficult to fulfil the selective degradation of chlorophenol contaminants. Therefore, the exploration of new catalysts to treat chlorophenol is necessary.

Nowadays, the metallic nanostructures featured with evident surface plasmon resonance (SPR) have become good candidates for the photodegradation of organic contaminants.[15,16] Among these plasmonic photocatalysts, Ag/AgCl materials have been the focus of attention,[17–22] because they exhibit remarkable resonant behaviour when interacting with ultraviolet (UV) and visible (vis) photons through an excitation of SPR.[23] Up to now, Ag@AgCl nanoparticles (NPs),[24,25] Ag/AgCl nanocubics,[26] and Ag/AgCl-based nanocomposites[27] have been investigated for the development of plasmonic photocatalysts and the application to the degradation of organic contaminants. In addition, offering large surface areas, three dimensional (3D) network-structures can not only offer excellent performance for the reaction, which is the result of the existence of fertile active sites for the catalysis such as corners, edges and steps[28–32] but can also greatly facilitate reactant diffusion and transportation. However, there is neither report about the network-structured Ag/AgCl nanocomposites, and nor on the use of composite for the selective-degradation of chlorophenol compounds. Consequently, it remains a great challenge for the launch of an efficient route for the synthesis of network-structured Ag/AgCl nanocomposites and employment as plasmonic photocatalysts to selectively degrade refractory chlorophenol contaminants.

In this work, 3D Ag/AgCl network-nanostructure in which the average diameter of the network nanowires (NWs) is ~20 nm and pore channels have a narrow macropore distribution from 50 to 100 nm, were synthesized based on Ag NWs or nanospheres template through the element lithographic network construction (ELNC) process. Used as plasmonic photocatalysts, they could exhibit considerably higher catalytic performance and better stability for the selective-

[a]*Department of Chemistry, Key Laboratory of Yangtze River Water Environment, Ministry of Education, Tongji University, 1239 Siping Road, Shanghai 200092, China. E-mail: m_wen@tongji.edu.cn; Fax: +86-21-65981097*

[b]*Shanghai Key Laboratory of Chemical Assessment and Sustainability, Tongji University, Shanghai 200092, China*

† Electronic supplementary information (ESI) available: Further details SEM images, XRD pattern, EDS data, UV-visible diffuse reflectance spectrum, and UV-vis absorption spectra of as-prepared catalysts for the degradation of 4-CP. See DOI: 10.1039/c4ra14459g

degradation of 4-CP, compared with commercially available P25-TiO_2 under UV-light irradiation. The formulated Ag/AgCl network-structures could be good candidates for organic pollutant elimination. The proposal formation mechanism, reaction activity and reusability were investigated in detail in this work.

Results and discussion

Network-structured Ag/AgCl plasmonic photocatalysts were synthesized through the ELNC process based on Ag NWs or nanospheres template. Ag NWs were prepared in an improved ethylene glycol process by employing the long-chain PVP (K90, MW = 800 000) as structure directing agent. The synergistic interaction between the carbonyl groups on the long-chain PVP macromolecule and silver ions results in the one-dimensional (1D) structure. As shown in Fig. 1, based on the template of the as-prepared Ag NWs, the etching agent of $CuCl_2$ was introduced into the reaction system. Then, AgCl NPs were generated on the surface of the Ag NWs by integration between Ag^+ and Cl^-. Moreover, Cu^{2+} can be attracted to the surface of Ag NWs by electrostatic interaction. Because the standard reduction potential (SHE) of the Cu^{2+}/Cu redox couple is 0.34 V, which is higher than that of the AgCl/Ag redox couple (0.22 V *vs.* SHE), thus some Ag atoms from Ag NWs were oxidized to Ag^+ by Cu^{2+} ($Ag^+ + Cl^- \rightarrow AgCl$), and generated AgCl coupled with Ag companying with the formation of large amount of the porous channels. This ELNC process finally leads to the formation of network-structured Ag/AgCl NWs. In addition having firm frame support for the active sites, Ag/AgCl network-structures can offer large surface area and reaction performance chambers, which prefers to facilitate reactant diffusion and transport. If long-chain PVP is replaced by a short one (K30, MW = 580 000), network-structured Ag/AgCl nanospheres can be acquired from Ag nanospheres. The formation process was monitored by field-emission scanning electron microscopy (FESEM), X-ray diffraction (XRD) patterns and energy dispersive X-ray spectroscopy (EDS) analysis (Fig. S1†). In this reaction system, the reaction temperature and solvent are important factors for the fabrication of Ag/AgCl network structures (Fig. S2 and S3†). The Ag/AgCl network-nanostructures with well distributed macropores can only be prepared at 170 °C in ethylene glycol.

Fig. 2 presents the FESEM and TEM characterization for Ag/AgCl network-nanostructures. The mean diameter of the sacrificial template Ag NWs is ~500 nm (Fig. 2A). As-synthesized 1D Ag/AgCl network-structures consist of the network NWs at the average diameter of ~20 nm and the pore channels at narrow macropore distribution from 50 nm to 100 nm (Fig. 2B and C). A distinct contrast of network NWs and pore channels can be clearly observed in the TEM image in Fig. 1D, the dark is network Ag/AgCl NWs and the white interstices are pore channels. Similarly, the morphology of Ag/AgCl nano-networks fabrication from Ag nanospheres is shown in Fig. 2E–H. The average size of Ag/AgCl network-structured nanospheres and the Ag nanospheres are both ~500 nm. The diameters of the network NWs and the pore channel distribution are the same size as that of 1D Ag/AgCl network-structures fabricated from Ag NWs, which is due to the preparation under exactly the same condition, except PVP. Fig. 2I shows typical HRTEM images of the Ag NWs template. The fringe spacing of 0.21, 0.24 and 0.34 nm can be indexed to the (111), (200) and (220) planes, respectively, of face-centered cubic (fcc) Ag. The selected area electron diffraction (SAED) pattern from the same Ag NWs (Fig. 2J) exhibits a single crystal diffraction pattern with the indexed plane of $(\bar{1}1\bar{1})$, (220) and $(\bar{2}00)$. The HRTEM image in Fig. 2K shows the Ag/AgCl network-structures with the lattice spacing of 0.18 and 0.24 nm, corresponding to the AgCl (200) and Ag (200) planes, respectively. The SAED pattern for Ag/AgCl network-structures illustrates a clear crystalline spot ring (Fig. 2L), which corresponds to the polycrystalline structure with the indexed plane of AgCl (200), (111) and (220) and Ag $(\bar{1}1\bar{1})$, indicating the formation of Ag/AgCl network-structures.

Fig. 3 shows the typical XRD patterns of the as-synthesized Ag NWs and Ag/AgCl network-structured NWs. Compared to that of pure Ag NWs, distinct diffraction peaks (2θ) at 27.8° (111), 32.3° (200), 46.3° (220), 54.9° (311) and 57.5° (222) could be unambiguously detected. These diffraction peaks are attributed to the typical cubic phase of AgCl (JCPDS no. 31-1238). At 38.1°, 44.4° and 64.2°, some diffraction peaks can also be found, which are consistent with the (111), (200) and (220)

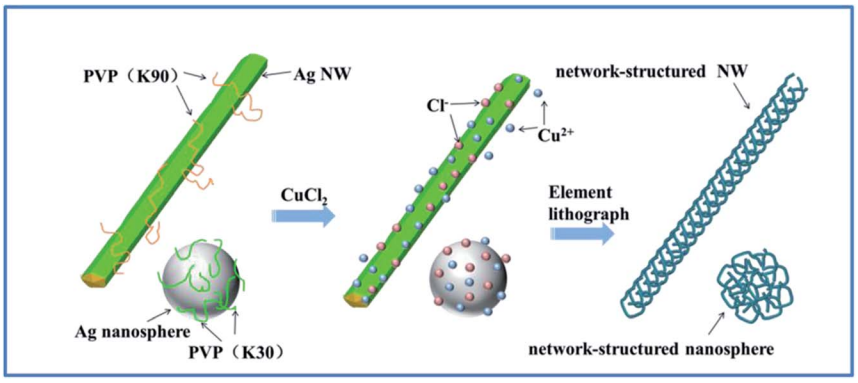

Fig. 1 Schematic view of the procedure for the construction of Ag/AgCl network-nanostructures based on Ag NW and nanosphere *via* ELNC process.

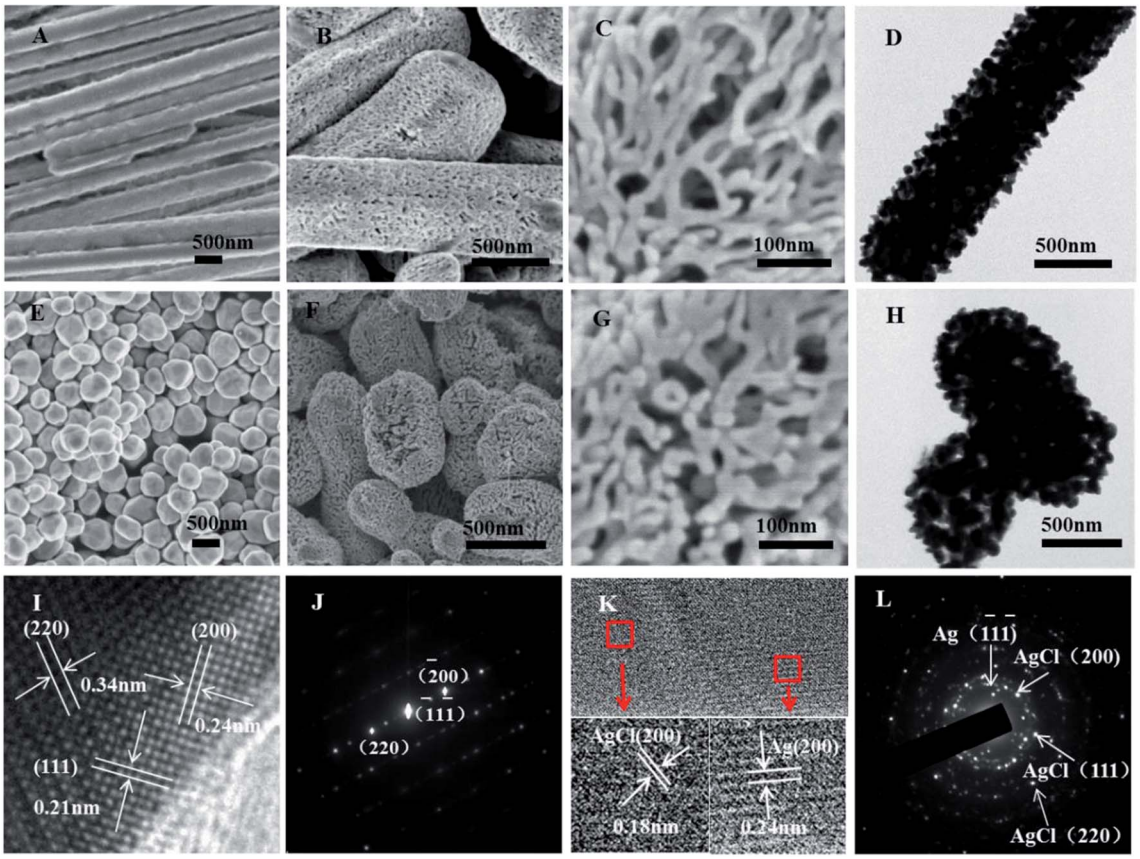

Fig. 2 SEM images of Ag NWs (A) and Ag nanospheres (E); SEM images of network-structured Ag/AgCl NWs (B and C) and nanospheres (F and G); TEM images of Ag/AgCl network-structured NWs (D) and nanospheres (H); HRTEM images and SAED patterns of Ag NWs (I and J) and network-structured Ag/AgCl NWs (K and L).

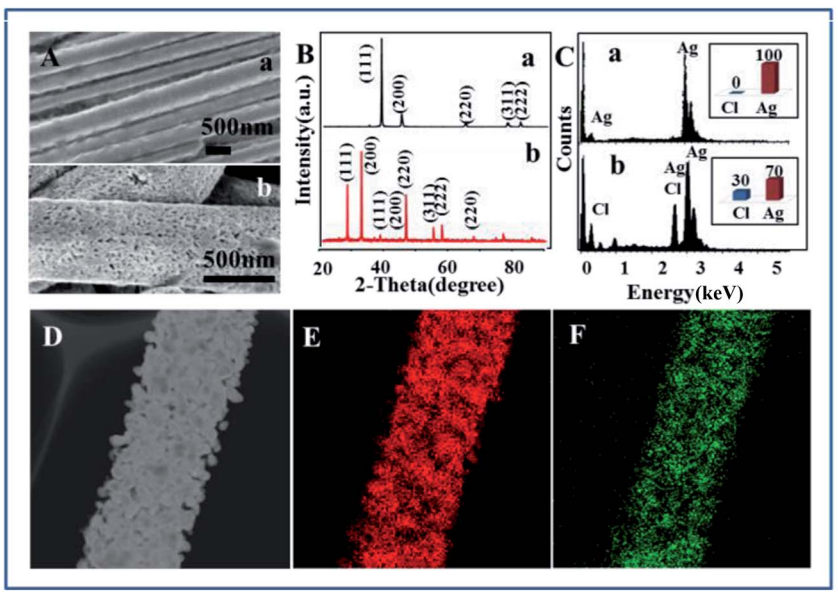

Fig. 3 SEM images (A), XRD patterns (B) and EDS analysis with inset of element accounts (C) of Ag NWs (a) and Ag/AgCl network-structured NWs (b); elemental maps for Ag (E) and Cl (F) of a single sparse Ag/AgCl network-structured NW (D).

planes of Ag with a face-centered cubic structure (JCPDS no. 01-1167). EDS analysis was adopted to determine the components of the network nanostructures. As shown in Fig. 3C, the atomic ratio of Ag : Cl is approximately 7 : 3, which is considerably higher than the theoretic stoichiometric atomic ratio of 1 : 1 for Ag : Cl in AgCl. It indicates that the Ag elements of the higher part one exist in the form of elementary Ag, and the mole ratio between Ag and AgCl is approximately 4 : 3 in these network nanostructures. In order to clearly understand the elemental distribution of the as-designed network structures, a single sparse Ag/AgCl network-structured NW is characterized by bright field scanning TEM (BF-STEM). Fig. 3D shows a representative STEM image. Fig. 3E and F illustrate the corresponding EDS maps for Ag and Cl, in which the content of Ag is considerably higher than Cl, confirming that the products are Ag/AgCl network-structured NWs.

The XPS spectra of Ag NWs and network-structured Ag/AgCl NWs samples are presented in Fig. 4, in which the numbers of emitted photoelectrons are given as a function of the binding energy up to 800 eV. It can be observed that the Ag NWs present three photoemission peaks (Ag 3d, C 1s and O 1s) in Fig. 4A. Moreover, another peak of Cl 2p appears in the Ag/AgCl network-nanostructures in Fig. 4B. Magnified Ag 3d peaks in Fig. 4C, which consist of two sharp peaks 368.2 and 374.2 eV, are owing to the spin–orbit splitting of $3d_{5/2}$ and $3d_{3/2}$, respectively. These peaks could be further separated into two peaks. 367.5, 368.4 eV could be attributed to the Ag^{+} of AgCl, and 373.5, 374.4 eV could be ascribed to Ag^{0}. The semiquantitatively calculated surface mole ratio Ag : AgCl is approximately 4 : 3. These results matched well with the information from the element analysis. For Cl^{-}, the magnified Cl 2p peaks, which consist of two sharp peaks 199.6 and 198.0 eV, are due to the spin–orbit splitting of $2p_1$ and $2p_3$, respectively (Fig. 4D).

The UV-vis diffuse reflectance spectra of as-prepared Ag/AgCl network-structured NWs and nanospheres, as well as commercial P25-TiO_2, which was used as our reference photocatalyst, are compared and shown in Fig. S4 in ESI.† In contrast to P25-TiO_2 NPs, the Ag/AgCl network-structured nanocomposites have a strong absorption in the visible region due to the plasmon resonance of Ag NPs in the network nanostructures. The reason suggested is that a wavelength of light is much greater than the diameter of Ag NP, the electromagnetic field across the entire Ag NP is essentially uniform. As the electromagnetic field oscillates, the weakly bound electrons of the Ag NP respond collectively, giving rise to a plasmon state. When the incident light frequency matches the plasmon oscillation frequency, light is absorbed, resulting in surface plasmon absorption. The NPs consisting of Ag/AgCl network structures have a large number of different shapes and diameters so that their plasmon oscillation cover a wide range of frequencies,[33,34] and hence Ag/AgCl can absorb in a wide range of UV- and vis- light. Therefore, network Ag/AgCl nanostructures have excellent photocatalytic performance in visible light toward organic dyes, but as for chlorophenol, photodegradation under visible light is quite difficult to realize, even numbers of catalysts cannot do it under UV irradiation.

The photocatalytic performance and selectivity of as-synthesized catalysts were investigated in terms of the photodegradation of 4-CP under UV-light irradiation, and shown in Fig. 5. In order to exclude the possibility that the degradation of 4-CP was caused by the UV-light irradiation, a blank experiment was carried out where only 4-CP without any photocatalyst was involved (Fig. S5†). It can be proven

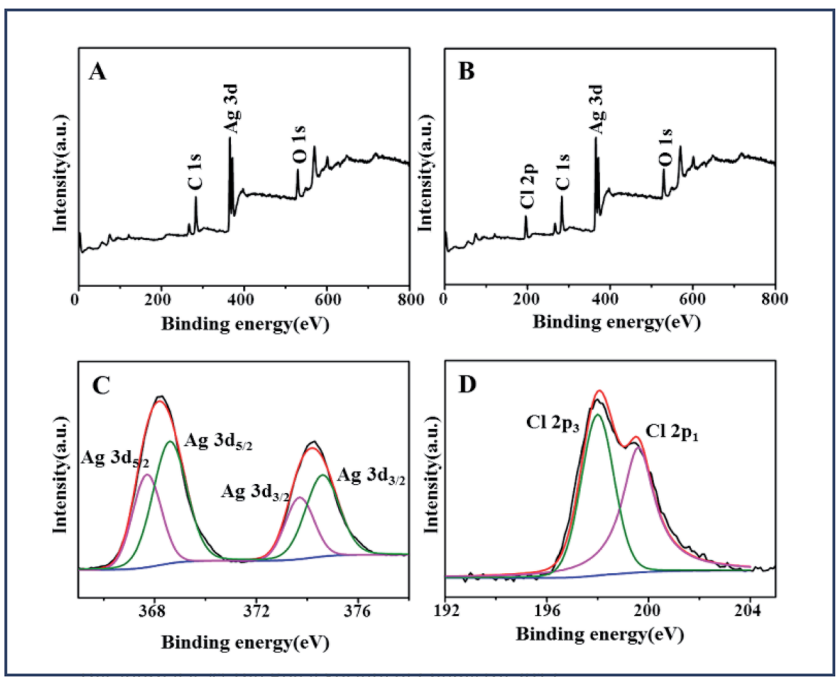

Fig. 4 XPS analysis of Ag NWs (A) and network-structured Ag/AgCl NWs (B) with the detailed spectra of Ag 3d (C) and Cl 2p (D).

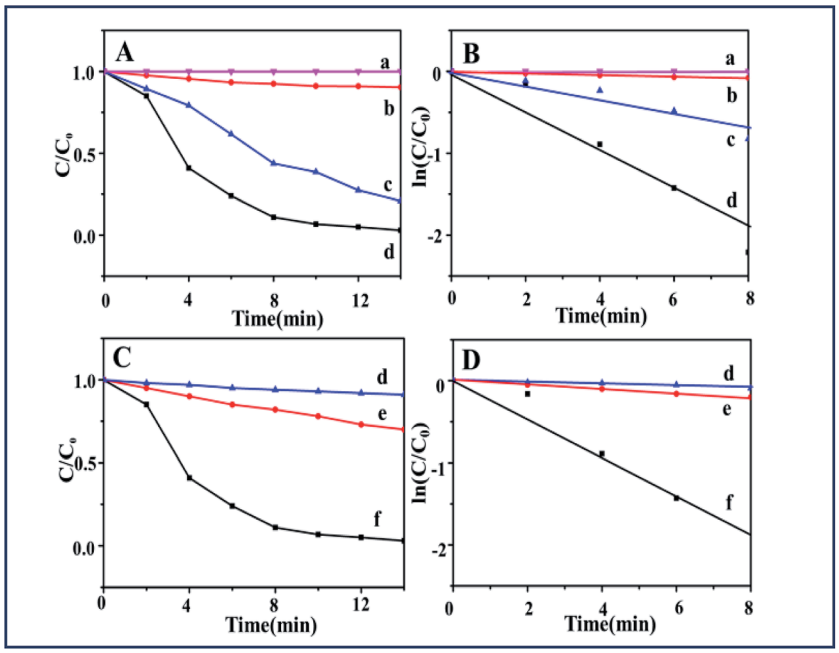

Fig. 5 (A and B) Plots of C/C_0 and $\ln(C/C_0)$ *versus* time for the photodegradation of 4-CP by Ag NWs (a), commercial P25-TiO_2 (b), network-structured Ag/AgCl NWs (c) and network-structured Ag/AgCl nanospheres (d); (C and D) plots of C/C_0 and $\ln(C/C_0)$ *versus* time for the photodegradation of 2-CP (d), 3-CP (e) and 4-CP (f) by using network-structured Ag/AgCl nanospheres as catalysts under UV-light at r.t.

that the irradiation does not degrade 4-CP in the absence of catalysts. To compare the photocatalytic performance of different catalysts, 4-CP was catalytically degraded by different catalysts, including Ag NWs, P25-TiO_2, network-structured Ag/AgCl NWs and nanospheres (Fig. 5A and B), and their UV spectra are illustrated in Fig. S6.† As shown in Fig. 5A, when Ag NWs are involved in the reaction system, the photodegradation of 4-CP can be negligible under UV irradiation. This can suggest that the self-photo-sensitized decomposition of 4-CP under our experimental conditions can basically be ignored. While network-structured Ag/AgCl nanospheres and NWs were used as photocatalysts, 90% and 80% degradation of 4-CP could be achieved, respectively, whose photocatalytic performance are much higher than that (5%) of commercially available P25-TiO_2. Compared with network-structured Ag/AgCl NWs, network-structured Ag/AgCl nanospheres display a significant advantage, which is attributed to the large surface areas and fertile active sites based on the same content of AgCl (Table S1†). As plotted in Fig. 5B, there is a nice linear correlation between $\ln(C/C_0)$ and the reaction time (t). It indicates that the photodecomposition reaction of 4-CP molecules, photocatalyzed by our catalysts, can be treated as a pseudo-first-order reaction. The rate constant (k) of the photocatalytic degradation of 4-CP over network-structured Ag/AgCl nanospheres is determined to be 0.28 min^{-1}, which is distinctly higher than that (0.10 min^{-1}) of network-structured Ag/AgCl NWs.

Meanwhile, the selective-catalytic-degradation performances of network-structured Ag/AgCl nanospheres are evaluated toward the photodegradation of chlorophenol, including 2-CP, 3-CP and 4-CP. As shown in Fig. 5C, when network-structured Ag/AgCl nanospheres are involved in the reaction system, nearly 90% conversion can be achieved for 4-CP, while only about 30% and 10% conversions are given for 3-CP and 2-CP, separately. It exhibits the selectivity of the catalysts of network-structured Ag/AgCl nanospheres, which prefer to catalyse the degradation of 4-CP. The reason is suggested to be caused by the steric hindrance, which is an important factor for the catalytic reaction performance. The steric hindrance for the three catalytic substrates decreases in the order of: 2-CP > 3-CP > 4-CP, which is opposite of the order of the photocatalytic activity. Therefore, steric hindrance can affect the absorption of catalysts to the catalytic substrates. Fig. 5D plots a nice linear correlation between $\ln(C/C_0)$ and the reaction time (t), and can be treated as a pseudo-first-order reaction. The rate constants (k) of the photocatalytic degradation of 2-CP and 3-CP over network-structured Ag/AgCl nanospheres are determined to be 0.011 min^{-1} and 0.025 min^{-1}, respectively.

As it is known, besides the catalytic activity, the recyclability of the catalysts is another principle substantially required by high-quality catalytic species. The stability of our network-structured Ag/AgCl plasmonic photocatalysts was also evaluated on the basis of performing the 4-CP degradation reactions repeatedly, several times. As observed in Fig. 6, the catalysis performance decreased slightly after the sixth time. After the sixth catalysis routine, the morphology of the catalysts could still be kept completely, only a little structural collapse occurred in the catalytic process, which can be seen in the monitored SEM image (Fig. S7†). Thus, the as-designed

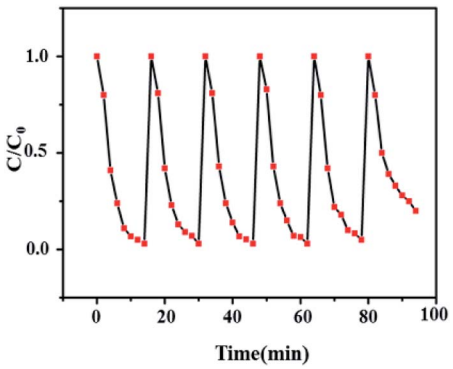

Fig. 6 Recyclability of photocatalytical degradation toward 4-CP catalyzed by network-structured Ag/AgCl nanospheres.

network-structured Ag/AgCl nanocomposites have excellent stability in the catalytic degradation of 4-CP.

Conclusions

A special Ag/AgCl network-nanostructure was synthesized based on Ag NW or nanosphere templates through the ELNC process. Offering large surface areas and many reaction performance chambers, the formulated Ag/AgCl network-nanostructures not only can provide firm frame support for the active sites, but also greatly facilitate reactant diffusion and transport. They could be used as high-performance yet durable UV-driven plasmonic photocatalysts for the selective-photodegradation of 4-CP. Compared with the commercially available P25-TiO_2 NPs, 3D Ag/AgCl network nanostructures exhibited much higher photocatalytic performance, suggesting the good potential application for organic pollutant elimination.

Experimental

Chemicals

Copper(II) chloride dihydrate ($CuCl_2 \cdot 2H_2O$, 99%), ethyl alcohol absolute (C_2H_5OH, 99%), silver nitrate ($AgNO_3$, 99.8%), ethylene glycol (EG, 99%), polyvinyl pyrrolidone (PVP, K30, MW = 58 000; K90, MW = 800 000) were all purchased from Sinopharm Chemical Reagent Co., Ltd. (SCRC). 2-Chlorophenol (C_8H_9ClO, 99%), 3-chlorophenol (C_8H_9ClO, 98%) and 4-chlorophenol (C_8H_9ClO, 99%) were purchased from Alfa Aesar. P25-TiO_2 (*ca.* 80% anatase and 20% rutile) nanospecies were purchased from Degussa and used as the reference photocatalysts for comparison. All the reagents were used without further purification.

Preparation

The method was improved from that of Kan's group, which was used to obtain Ag NWs.[35] In a typical synthesis of 3D network-structured Ag/AgCl plasmonic photocatalysts, 0.204 g $AgNO_3$, 0.204 g $CuCl_2 \cdot 2H_2O$ and 0.1332 g PVP (111 mg mL^{-1}, K90) were, respectively, dispersed in 10 mL of EG solution by sonication for 30 min, meanwhile, 10 mL EG solvent was magnetically stirred at 170 °C in a round-bottom flask. Then both $AgNO_3$ and PVP solutions were simultaneously injected drop-wise into the heated EG solution over a period of 5 min and kept for 80 min. And Ag NWs were obtained. Afterward, 10 mL 1.2×10^{-3} M $CuCl_2$ of EG solution was added to the mixture, in drops, in order to acquire network-structured Ag/AgCl NWs. The reaction stopped after 40 min when the mixtures turned slightly purple. Magnetic stirring was applied throughout the entire process. After the system was cooled to room temperature, the resulting products were collected by centrifuge and washed with ethanol and deionized water, several times, followed the drying treatment under vacuum for further characterization. If PVP (K90) was taken place by PVP (K30), network-structured Ag/AgCl nanospheres could be acquired from Ag nanospheres.

Photocatalytic test

To compare the photodegradation ability among the as-prepared Ag NWs, network-structured Ag/AgCl NWs, network-structured Ag/AgCl nanospheres and the commercial P25-TiO_2, the degradation of 4-CP (20 mg L^{-1}) solution is used to evaluate the photocatalytic activities of the prepared catalysts. The photocatalytic tests were performed in a reactor equipped with a cooling water-cycle system to keep the temperature stable. A 300 W mercury lamp was employed as the light source to produce UV irradiation. In a typical photocatalytic experiment, 30 mg Ag/AgCl were dispersed in 60 mL aqueous solution of 4-CP by sonication for 10 min, and the obtained suspension was magnetically stirred in the dark for 30 minutes to achieve adsorption–desorption equilibrium. During illumination, 2.0 mL suspension was withdrawn from the reactor every 2 minutes, followed by centrifugation and filtration, and the obtained clear solution was analyzed by ultraviolet spectroscopy. The concentration of 4-CP in the obtained sample was determined by detecting the absorption at 279 nm. Furthermore, to investigate the selective-catalytic-degradation performances of as-prepared network Ag/AgCl nanospheres, 2-CP, 3-CP and 4-CP, photodegradation were also investigated under the same condition.

Characterization

The morphology and structure of the samples were investigated by FE-SEM (JEOL, S-4800, Japan), TEM and HRTEM (JEOL JEM-1200EX microscope, Japan). The elemental distribution and elemental mapping were carried out by STEM under the BF mode on a JEOL JEM-2100 F microscope. Element analysis was conducted by EDS conducted at 20 keV on a TN5400 EDS instrument (Oxford). XRD patterns were recorded by using a Bruker D8 (German) diffractometer with a Cu Kα radiation source ($\lambda = 0.154056$ nm). XPS measurements were performed on a RBD-upgraded PHI-5000C ESCA system (Perkin Elmer) using Al Kα radiation ($h\nu = 1486.6$ eV). The whole XPS spectrum (0–800 eV) and the narrower, high-resolution spectra were all recorded using a RBD 147 interface (RBD Enterprises, USA). Binding energies were calibrated using the containment carbon (C 1s = 284.6 eV). UV-vis spectra of the samples were measured on an Agilent-8453 ultraviolet visible

spectrophotometer. UV-vis diffuse reflectance spectra of the samples were obtained on an UV-vis spectrophotometer (Hitachi U-3010) using $BaSO_4$ as the reference.

Acknowledgements

This work is financial supported by National Natural Science Foundation (no. 21171130, 51271132, 21471114, and 91222103) and 973 Project (no. 2011CB932404) from China.

Notes and references

1 A. S. Cherevan, P. Gebhardt and C. J. Shearer, *Energy Environ. Sci.*, 2014, **7**, 791–796.
2 R. G. Li, H. X. Han and F. X. Zhang, *Energy Environ. Sci.*, 2014, **7**, 1369–1376.
3 C. Catrinescu, D. Arsene and C. Teodosiu, *Appl. Catal., B*, 2011, **101**, 451–460.
4 O. Legrini, E. Oliveros and A. M. Braun, *Chem. Rev.*, 1993, **93**, 671–698.
5 H. Tada, T. Kiyonaga and S. Naya, *Chem. Soc. Rev.*, 2009, **38**, 1849–1858.
6 C. C. Chen, W. H. Ma and J. C. Zhao, *Chem. Soc. Rev.*, 2010, **39**, 4206–4219.
7 L. H. Wang, L. Xu and Z. X. Sun, *RSC Adv.*, 2013, **3**, 21811–21816.
8 D. S. Bhatkhande, V. G. Pangarkar and A. A. C. M. Beenackers, *J. Chem. Technol. Biotechnol.*, 2002, **77**, 102–116.
9 M. R. Hoffmann, S. T. Martin and W. Choi, *Chem. Rev.*, 1995, **95**, 69–96.
10 A. Mills, R. H. Davies and D. Worsley, *Chem. Soc. Rev.*, 1993, **22**, 417–425.
11 D. Q. Zhang, G. S. Li and J. C. Yu, *J. Mater. Chem.*, 2010, **20**, 4529–4536.
12 X. B. Chen and S. S. Mao, *Chem. Rev.*, 2007, **107**, 2891–2959.
13 A. L. Linsebigler, G. Q. Lu and J. T. Yates, *Chem. Rev.*, 1995, **95**, 735–758.
14 A. Fujishima, T. N. Rao and D. A. Tryk, *J. Photochem. Photobiol., C*, 2000, **1**, 1–21.
15 C. Hu, Y. Q. Lan and J. H. Qu, *J. Phys. Chem. B*, 2006, **110**, 4066–4072.
16 H. L. Jiang and Q. Xu, *J. Mater. Chem.*, 2011, **21**, 13705–13725.
17 J. Song, J. Roh and I. Lee, *Dalton Trans.*, 2013, **42**, 13897–13904.
18 M. S. Zhu, P. L. Chen and W. H. Ma, *ACS Appl. Mater. Interfaces*, 2012, **4**, 6386–6392.
19 J. Y. Chen, B. J. Wiley and Y. N. Xia, *Langmuir*, 2007, **23**, 4120–4129.
20 B. Cheng, Y. Le and J. G. Yu, *J. Hazard. Mater.*, 2010, **177**, 971.
21 A. Murugadoss, N. Kai and H. Sakurai, *Nanoscale*, 2012, **4**, 1280–1282.
22 B. Erdem, R. A. Hunsicker and G. W. Simmons, *Langmuir*, 2001, **17**, 2664–2669.
23 Y. P. Bi, S. X. Ouyang and J. Y. Cao, *Phys. Chem. Chem. Phys.*, 2011, **13**, 10071–10075.
24 M. Ramstedt and P. Franklyn, *Surf. Interface Anal.*, 2010, **42**, 855–858.
25 C. H. An, S. Peng and Y. G. Sun, *Adv. Mater.*, 2010, **22**, 2570–2574.
26 E. Kazuma, T. Yamaguchi and N. Sakai, *Nanoscale*, 2011, **3**, 3641–3645.
27 P. Wang, B. B. Huang and X. Q. Qin, *Angew. Chem., Int. Ed.*, 2008, **47**, 7931.
28 N. U. Silva, T. G. Nunes and M. S. Saraiva, *Appl. Catal., B*, 2012, **113–114**, 180–191.
29 Q. J. Xiang, J. G. Yu and B. Cheng, *Chem.–Asian J.*, 2010, **5**, 1466–1474.
30 M. Wen, M. Z. Cheng and S. Q. Zhou, *J. Phys. Chem. C*, 2012, **116**, 11702–11708.
31 B. L. Sun, M. Wen and Q. S. Wu, *Adv. Mater.*, 2012, **10**, 2860–2866.
32 M. Z. Cheng, M. Wen and S. Q. Zhou, *Inorg. Chem.*, 2012, **51**, 1495–1500.
33 P. K. Jain, W. Y. Huang and M. A. El-Sayed, *Nano Lett.*, 2007, **7**, 2080–2088.
34 H. C. Guo, N. Liu and L. W. Fu, *Opt. Express*, 2007, **15**, 12095–12101.
35 C. X. Kan, J. J. Zhu and X. G. Zhu, *J. Phys. D: Appl. Phys.*, 2008, **41**, 155304.